Am J Cancer Res 2022;12(7):3242-3258
www.ajcr.us /ISSN:2156-6976/ajcr0142512

*Original Article*

# MUC1 is responsible for the pro-metastatic potential of calycosin in pancreatic ductal adenocarcinoma

Wenqing Chen[1,2*], Zhu Zhang[1*], Ken Kin-Lam Yung[1], Joshua Ka-Shun Ko[2,3]

*[1]Department of Biology, Hong Kong Baptist University, Hong Kong SAR, China; [2]Teaching and Research Division, School of Chinese Medicine, Hong Kong Baptist University, Hong Kong SAR, China; [3]Centre for Cancer and Inflammation Research, School of Chinese Medicine, Hong Kong Baptist University, Hong Kong SAR, China. [*]Equal contributors.*

Received February 23, 2022; Accepted June 11, 2022; Epub July 15, 2022; Published July 30, 2022

**Abstract:** Pancreatic ductal adenocarcinoma (PDAC) is a prominent type of pancreatic cancer. We have recently unveiled that the anti-tumor adjuvant calycosin concurrently possesses growth-inhibitory and pro-metastatic potential in PDAC development by regulating transforming growth factor β (TGF-β), which plays dual roles as both tumor suppressor and tumor promoter. Hence, we are interested to explore if the pro-metastatic property of the drug could be attenuated for effective treatment of PDAC. Through network pharmacology, MUC1 had been identified as the most common drug target of herbal *Astragalus* constituents (including calycosin) in treating PDAC. Following MUC1 gene silencing, the drug effects of calycosin on migratory activity, growth and metabolic regulation of PDAC cells were assessed by using immunofluorescence microscopy, quantitative real-time polymerase chain reaction (qRT-PCR), Western immunoblotting, co-immunoprecipitation (Co-IP), wound healing assay and flow cytometry, respectively. Through *in vivo* experiments, we further validated the working relationship between MUC1 and TGF-β. Results have elucidated that MUC1 gene suppression could switch off the migratory and pro-metastatic drive of calycosin while retaining its growth-inhibitory power by inducing apoptosis and cell cycle arrest, as well as facilitating autophagy and metabolic regulation. The underlying mechanism involves downregulation of TGF-β that acts via modulation of AMP-activated protein kinase (AMPK), Sirtuin 1 (Sirt1) and fibroblast growth factor 21 (FGF21) signaling. These findings have provided new insights in the safe and target-specific treatment of PDAC.

**Keywords:** Calycosin, MUC1, pancreatic ductal adenocarcinoma, metastasis, TGF-β

## Introduction

Pancreatic cancer is a highly lethal malignancy with early metastatic property. The 5-year survival rate in pancreatic cancer patients is only 9%, being the lowest amongst other solid cancers with more than 57,600 newly diagnosed cases and causing 47,050 deaths in the U.S.A. in 2020, which has been estimated to become the second leading cause of cancer-related deaths in 2030 [1, 2]. Pancreatic ductal adenocarcinoma (PDAC) is the most common histologic type of pancreatic malignancy, comprising almost 90% of all malignant pancreatic neoplasms [3]. It is characterized by late diagnostic detection, rapid local spread, and the lack of reliable biomarkers and efficacious treatment schemes [4].

Calycosin is a bioactive isoflavonoid among the main ingredients of Radix Astragalus, a lead herb in various Traditional Chinese medicine formulations. It has been reported to possess antitumor, neuroprotective, anti-inflammatory, and proangiogenic properties [5]. Our research group has recently reported that calycosin could significantly inhibit the growth of PDAC cells through induction of cell cycle arrest and apoptosis, but concurrently increased cell migration and invasiveness due to the crucial involvement of TGF-β [6].

MUC1 is a heterodimeric transmembrane protein localized at the apical membranes of normal secretory epithelial cells, with frequent overexpression at the cancer cell surface [7-11]. In clinical practice, MUC1 has been used as a cancer biomarker to evaluate PDAC patient's survival rate [7]. A high expression level of MUC1 in cancer cells would promote cell growth, survival, migration, and invasion which are related to poor prognosis, while it

may also provoke energy metabolism [10, 12, 13]. Thus, MUC1 can be viewed as an oncogenic factor involved in a variety of signalling pathways including Wnt/β-catenin [14, 15], proto-oncogene tyrosine-protein kinase (c-Src) [16], growth factor receptor-bound protein 2 (Grb2)/son of sevenless (Sos) [17], phosphoinositide 3-kinase (PI3K)/Akt [7], p53 [18], glycogen synthase kinase-3 (GSK3) [19], epidermal growth factor receptor (EGFR) [20], nuclear factor kappa-light-chain-enhancer of activated B cells (NF-κB) [21], hepatocyte growth factor (HGF)/tyrosine-protein kinase Met (c-Met) [14], transforming growth factor β (TGF-β) [8, 15, 22], fibroblast growth factor 21 (FGF21) [23], mitogen-activated protein kinase (MAPK)/c-Jun NH2-terminal kinase (JNK)/activator protein 1 (AP-1) [13, 15] and janus kinase 2 (JAK2)/signal transducer and activator of transcription 3 (STAT3) [24]. MUC1 has also been known to have a close working relationship with TGF-β in cancer cells [8] by switching its phenotype from tumor suppressor to tumor promoter in pancreatic cancer development [25]. In the present study, we hypothesize that through MUC1 modulation, the pro-metastatic potential of calycosin in PDAC via TGF-β signaling would be attenuated while preserving its growth-inhibitory tumor suppressor property.

## Materials and methods

### *Collection of common gene targets of Astragalus constituents and PDAC*

The pharmacological genes of PDAC were obtained from TTD (Therapeutic Target Database), DisGeNET and OMIM (Online Mendelian Inheritance in Man), while the disease-conditioning genes of *Astragalus* constituents were collected from the TCMIDZ (Traditional Chinese Medicines Integrated Database) and NPASS (Natural Product Activity and Species Source database) database. Subsequently, identified genes were pooled before obtaining the therapeutic targets of *Astragalus* constituents in treating PDAC to obtain a Venn diagram of the potential targets of calycosin.

### *Network target construction and analysis of Astragalus constituents in treating PDAC*

The web-available STRING database was accessed for analysis of pooled therapeutic targets of *Astragalus* constituents in treating PDAC, followed by identification of the interrelated network proteins. Following this, the system PPI networks with all core targets were created, resulting from the reference data greater than 0.9 using Cytoscape software. Besides, topological indexes following Network Analyzer were screened and determined for the identification of core targets.

### *Reagents*

Calycosin (CAS no. 20575-57-9; >98% purity by HPLC) was purchased from Chengdu Herbpurify Co., Ltd. (Chengdu, Sichuan, China). The stock solution of the drug was prepared by dissolving in 0.1% dimethylsulfoxide (DMSO). Silencer™ Select Muc1 siRNA (4392420) and Silencer™ Select Negative Control No. 2 siRNA (4390846) were purchased from Thermo-Fisher Scientific (Waltham, MA, USA). They were resuspended in nuclease-free water with the final working concentration of 50 nmol. Annexin V/propidium iodide (PI) staining kit was purchased from BD Biosciences (San Jose, CA, USA). FxCycle TM PI/RNase staining solution was purchased from Invitrogen (Carlsbad, CA, USA). The following antibodies were used in the IF assay: Primary - MUC1-CT (ab109185, Abcam); TGF-β1 (ab64715, Abcam); pAMPKα (2531, Cell Signaling Technology). Secondary - IgG (H+L) cross-adsorbed goat anti-mouse, goat anti-rabbit IgG (H+L) cross-adsorbed secondary antibody, rabbit IgG (H+L) cross-adsorbed secondary antibody (all obtained from Alexa Fluor™ 546, Invitrogen™, Thermo Fisher Scientific). The following antibodies were used for Western immunoblotting: Primary - MUC1 was purchased from Santa Cruz Biotechnology (sc7313, CA, USA); TGF-β1 (3711), Snail (3879), Cleaved-PARP (9541) and Atg5 (2630) were all purchased from Cell Signaling Technology (CST, CA, USA). Secondary - goat anti-mouse IgG-HRP and goat anti-rabbit IgG-HRP were purchased from Santa Cruz Biotechnology (CA, USA).

### *Isolation, identification, and culture of PDAC cell lines*

Human pancreatic ductal adenocarcinoma (PDAC) cell MIA PaCa-2 was obtained from American Type Culture Collection (ATCC; Manassas, VA, USA). All cells were grown in Dulbecco's modified Eagle's medium (DMEM) supplemented with 10% fetal bovine serum (FBS) plus 1% penicillin and streptomycin. All chemicals for cell culture were purchased from

Thermo-Fisher Scientific (Waltham, MA, USA) unless specified otherwise. Cells were incubated at 37°C with 5% $CO_2$.

*3D cell culture*

3D tumor models retain important characteristics of *in vivo* tumors and can be used to review the detailed molecular signature and behavior of cancer cells. Suspended 3D cultures will be established from the above cancer cell lines as cancer spheroids. MIA-PaCa2 cells were seeded into at a density of 500 cells per well in 96-well Ultra-Low Attachment Multiple Well Plate (Corning) and cultured for 7 days using 10% FBS at 37°C with 5% $CO_2$. Then, every well would generate one spheroid.

*Drug treatments*

siRNA transfection was conducted to facilitate MUC1 gene knockdown in MIA-PaCa2 cells to investigate the influence on drug action of calycosin. MIA-PaCa2 cells were seeded at a density of $7\times10^5$ cells per well in 6-well plates using DMEM with 10% FBS. Following this, 5 μl of Lipofectamine® 2000 Transfection Reagent (Invitrogen™, Thermo Fisher Scientific) and 5 μl of either negative control (NCtrl) siRNA reagent or MUC1 siRNA reagent was separately diluted in 250 μl Opti-MEM medium for 5 minutes. Diluted Lipofectamine® 2000 Transfection Reagent was mixed with diluted NCtrl siRNA reagent or MUC1 siRNA reagent for another 20 minutes. The lipid complexes were then added to each well and the plate was incubated at 37°C with 5% $CO_2$ for 6 hours. Cells were then treated with calycosin (50 or 100 μmol) for 24 hours.

*Immunofluorescence (IF) assay*

For IF microscopic analysis, MIA-PaCa2 cells were fixed and probed with MUC1-CT (Abcam; 1:200 dilution) that specifically labelled its cytoplasmic C-terminal, TGF-β1 (Abcam; 1:200 dilution), pAMPKα (CST; 1:200 dilution) overnight at 4°C. Then, cells were washed and probed with the corresponding secondary antibody, followed by the addition of mounting medium containing 40,6-diamidino-2-phenylindole (Vector Laboratories). The images were captured by using a Zeiss LSM 710 confocal laser scanning microscope (Carl Zeiss, Inc., Thornwood, NY, USA).

*Co-immunoprecipitation (Co-IP) assay*

To perform the Co-IP assay, MIA-PaCa2 cells were divided into two groups. One group was the control group. The other group was the drug administration group (100 μM calycosin). MIA-PaCa2 cells were incubated with 100 μM calycosin for 24 hours, after which they were lysed. The lysate protein concentration was measured and the sample concentration in each group was controlled at 1 μg/μl. 50 μL of protein A+G magnetic beads (Beyotime) were incubated with anti-MUC1 or IgG antibodies for 30 min at room temperature. The beads were then mixed with the cell lysate overnight at 4°C. The complexes were eluted using Tris-buffered saline (TBS) and 50 μl 1× SDS loading buffer was added to each sample, followed by heating at 95°C for 5 min. The beads were then removed to collect the supernatant for subsequent Western blot analysis.

*Wound healing assay*

Cells were seeded in 6-well plates and cultured until reaching 90% confluence. siRNA transfection was performed for 6 hours. A line scratch was made with a 100-μl pipette tip before the first image was acquired. Calycosin in a 2% FBS medium was added to the cell culture for another 24 or 48 h, when the second and third images were obtained. Multiple views of each well were documented with each experiment repeated in triplicate.

*Reverse transcription-quantitative polymerase chain reaction (qRT-PCR)*

The total RNA of drug-treated cells was extracted by Quick-RNA Miniprep Kit (ZYMO Research). Gene expression data were normalized to β-actin. And the primers were listed in **Table 1**.

*Western blot analysis*

Western immunoblotting was used to determine the protein expression of MUC1, TGF-β1, Snail, Cleaved-PARP and Atg5. Drug-treated cells were lysed in RIPA buffer to extract the total protein. Protein samples were then separated by 8-12.5% SDS-PAGE and transferred to the PVDF membrane. The membrane was blocked in 5% milk blocking buffer for 1 h and incubated in the indicated antibodies overnight at 4°C. The membrane was then washed 3 times in TBST buffer and incubated in the sec-

**Table 1.** Primers sequences used for qRT-PCR are as follows

| Gene | FP (5' to 3') | RP (5' to 3') |
|---|---|---|
| MUC1 | CCTACCATCCTATGAGCGAGTA | ACTGCTGGGTTTGTGTAAGAG |
| TGF-β1 | GCCCTGGACACCAACTATTG | CGTGTCCAGGCTCCAAATG |
| Snail | TTCTCACTGCCATGGAATTCC | GCAGAGGACACAGAACCAGAAA |
| p21 | GCAGACCAGCATGACAGATTT | GATGTAGAGCGGGCCTTTGA |
| p27 | GATGTAGAGCGGGCCTTTGA | AGAAGAATCGTCGGTTGCAGG |
| AMPKα | CACAGAGATCGGGATCAGTTAG | GTGAGGTCACAGATGAGGTAAG |
| Sirt1 | AGTGGCAAAGGAGCAGATTAG | AGTGGCAAAGGAGCAGATTAG |
| FGF21 | ACCTGGAGATCAGGGAGGAT | GCACAGGAACCTGGATGTCT |
| β-Klotho | CCACCCTGGTTCTACTCTTATC | CCACCCTGGTTCTACTCTTATC |
| β-actin | TGGCACCCAGCACAATGAA | CTAAGTCATAGTCCGCCTAGAAGCA |

Primers were obtained from Bio-Dream Technology Co., Ltd. (Shenzhen, Guangdong, China) and Life Technologies Co., Ltd. (Kwai Chung, New Territories, Hong Kong).

ondary antibodies for another 1 h at room temperature. After washing three more times in TBST buffer, the relative density of each protein was quantified by using the Image J software and normalized by the housekeeping protein β-actin.

*Assessment of apoptosis*

After drug treatment for 24 h, MIA PaCa-2 cells were harvested by trypsin digestion, washed by PBS, and stained with Annexin V-fluorescein isothiocyanate (FITC) and PI according to the manufacturer's instructions. Samples were analyzed in a flow cytometer (FACS Canto™, Beckton Dickinson Biosciences, San Jose, CA). Early apoptotic cells were Annexin V-FITC positive and PI negative, while late-phase apoptotic cells (undergoing necrosis) were Annexin V-FITC and PI double-positive.

*Cell cycle analysis*

After drug treatment for 24 h, MIA PaCa-2 cells were harvested and fixed with ice-cold 70% ethanol at -20°C overnight. FxCycle™ PI/RNase was used for DNA staining according to the manufacturer's instructions. Samples were analyzed by flow cytometry to compute the percentage of cells at different phases of the cell cycle using the FlowJo software.

*Orthotopic tumor xenograft*

The animal experimentation protocols were pre-approved by the Research Ethics Committee of the Hong Kong Baptist University (REC/19-20/0107) and conducted under the Regulations of the Department of Health, Hong Kong SAR, China (Animal Licence) in accordance with the EU Directive 2010/63/EU and associated guidelines. Six-week-old male C57/BL6 mice were purchased from the Laboratory Animal Services Centre, The Chinese University of Hong Kong. The tumor model was established by subcutaneous inoculation of Pan02 cells ($1\times10^6$ cells per mouse) into the right flank of mice. Then, 6 days after inoculation, mice were randomly divided into four groups (n=8) as follows: Control group with medium injection (i.p.), the positive chemotherapeutic drug control group of gemcitabine 30 mg/kg (i.p.), calycosin 30 mg/kg treatment group (i.p.) and calycosin 30 mg/kg with electric gun treatment group (i.p.) to induce electroporation. All mice received drug treatments every day. The body weights and tumor diameters were measured every other day, and the tumor volume was calculated using the formula (short diameter) 2× (long diameter) ×0.5. At the end of the experiments, tumors were then excised and weighed. For the histological study, excised tumor specimens were fixed in 10% formalin and embedded in paraffin. Cryogenic sections of the tumor samples were then used for immunohistochemical (IHC) analysis.

*Immunohistochemical (IHC) analysis of animal tissues*

The excised tumor samples were embedded and fixed. Cryogenic tumor sections (5 μM) were prepared and stained with hematoxylin and eosin (H&E; Sigma-Aldrich, St. Louis, MO). IHC analysis for MUC1, MMP-2, MMP-9, TGF-β and CD31 was also performed. Representative areas were viewed under light microscopy (Nikon 90i, Tokyo, Japan) and photographed at a magnification of 20× for IHC, respectively.

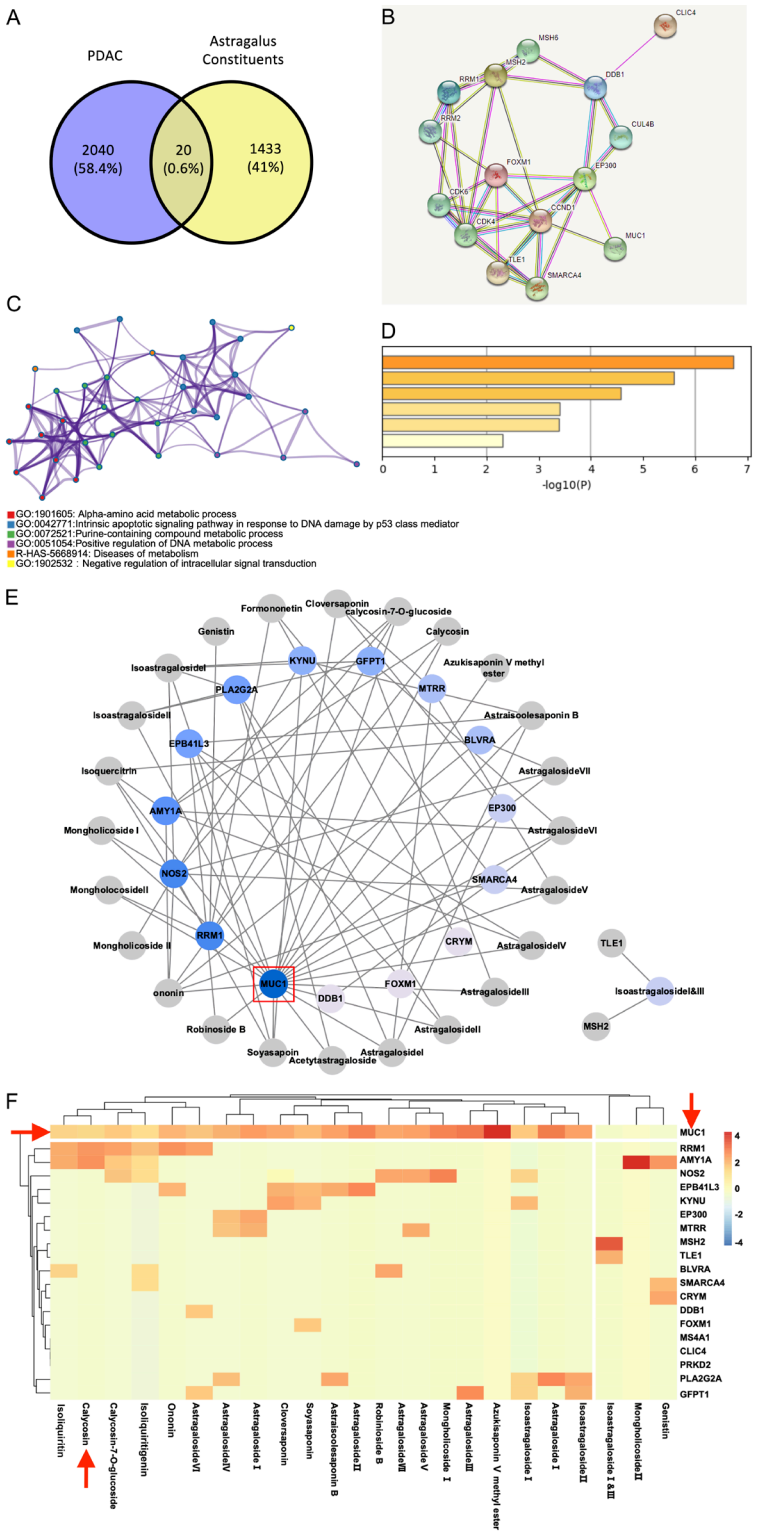


**Figure 1.** The Network Pharmacology analysis of PDAC and Astragalus constituents. A. Venn diagram of the potential gene targets of PDAC and *Astragalus* constituents. B. Protein-protein interaction (PPI) Network of the common potential gene targets. C. GO enrichment analysis of the common potential gene targets. D. Network layout of GO enrichment analysis. E. Cytoscape Network of common potential gene targets between PDAC and *Astragalus* constituents. F. Heatmap of common potential gene targets between PDAC and *Astragalus* constituents.

*Statistical analysis*

Numerical data are expressed as mean ± standard deviation (SD). Statistical significance of at least $P<0.05$ was determined by one-way analysis of variance (ANOVA) using GraphPad Prism 8.0 software followed by the Dunnett post-hoc test.

## Results

*Common targets of PDAC and Astragalus constituents by using network pharmacology*

To assess all the potential common targets between PDAC and *Astragalus* constituents, 2040 well-established PDAC-related genes were collected from the web-available databases of Therapeutic Target Database, DisGeNET, and OMIM. Besides, 1433 disease-conditioning genes of *Astragalus* constituents were also collected from the TCMID and NPASS database. Then, 20 potential common gene targets were filtered (**Figure 1A**). A PPI network (The Protein-Protein Interactions Network) was then established (**Figure 1B**) by String Database to visualize the inner relationship between the 20 filtered potential common gene targets. In the network map: pink lines indicate experimentally determined data; green lines represent targets that are adjacent to each other in space; red lines represent a fusion of the targets; blue lines represent simultaneous effects of the targets; yellow line represents the relationship between the targets obtained through text mining; black line represents co-expression of the target; purple line represents the protein homology. These results have shown that *Astragalus*

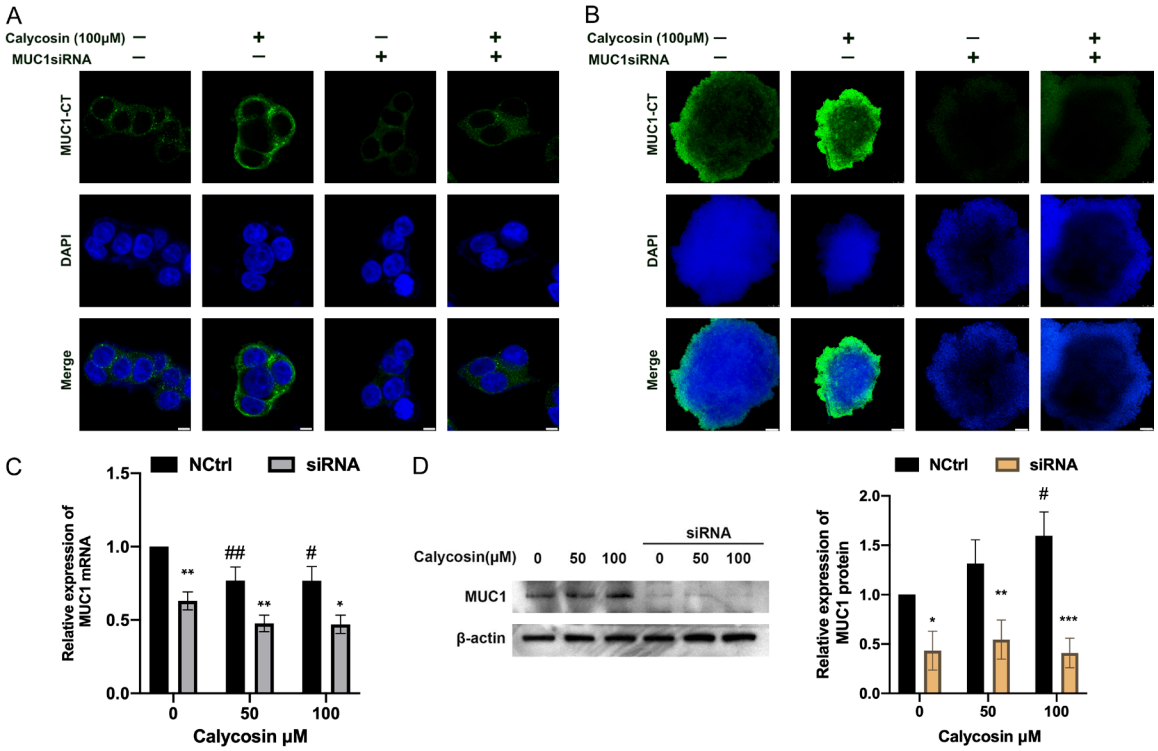


**Figure 2.** Effects of calycosin on the expression of MUC1 (with or without MUC1 gene silencing). Immunofluorescence staining of MUC1 (green) in MIA-PaCa2 cells treated with 100 μM calycosin for 24 h using (A) 2D or (B) 3D cell culture. The nuclei were stained with DAPI (blue). Magnifications: 60× for 2D cell culture (scale bar is 5 μm); 20× for 3D cell culture (scale bar is 50 μm). (C) Gene expression of MUC1 in MIA PaCa-2 cells after treatment with calycosin (50 or 100 μM) for 24 h was detected by quantitative reverse transcription PCR. $^{*}$P<0.01, $^{**}$P<0.0001 versus the corresponding negative control (NCtrl) group. $^{\#}$P<0.001, $^{\#\#}$P<0.0001 versus corresponding group without calycosin treatment (0 μM). (D) Protein expression of MUC1 in MIA PaCa-2 cells after treatment with calycosin (50 or 100 μM) for 24 h was detected by Western immunoblotting. $^{*}$P<0.05, $^{**}$P<0.01, $^{***}$P<0.001 versus the corresponding negative control (NCtrl) group. $^{\#}$P<0.05 versus corresponding group without calycosin treatment (0 μM). Cells treated with DMSO were used as negative control. Data are expressed as mean ± SD from 3 independent experiments.

constituents have the characteristics of possessing multiple targets in the treatment of pancreatic cancer. Besides, there is a synergy between multiple targets. GO analysis (**Figure 1C**, **1D**) of these common targets obtained from the Metascape platform has also been shown, of which most of them are related to metabolic regulation.

*MUC1 is the most correlated effector gene between PDAC and calycosin*

To further determine which target is the most effective one, the drug-gene network was established according to the duplicate value by using the Cytoscape software, (**Figure 1E**, **1F**). Data has indicated that MUC1 gene is the most potential relative biological target of *Astragalus* constituents in PDAC treatment. A heatmap was obtained to illustrate the correlation between each target and individual *Astragalus* constituents. MUC1 had been further verified as the most correlated drug target, including that of calycosin.

*Calycosin upregulated MUC1 expression in MIA-PaCa2 PDAC cells*

Based on our previous published data, we set the calycosin administration concentrations at 50 μM and 100 μM [6]. To explore the effect of calycosin on the expression of MUC1 in MIA-PaCa2 cells, immunofluorescence (IF) microscopy was performed in both 2D and 3D cell cultures (**Figure 2A**, **2B**). MUC1 expression was upregulated after calycosin treatment (100 μM) for 24 h in both 2D and 3D cultures, whereas the expression signal became extremely weak following MUC1 gene silencing. Results from qRT-PCR indicate that MUC1 gene ex-

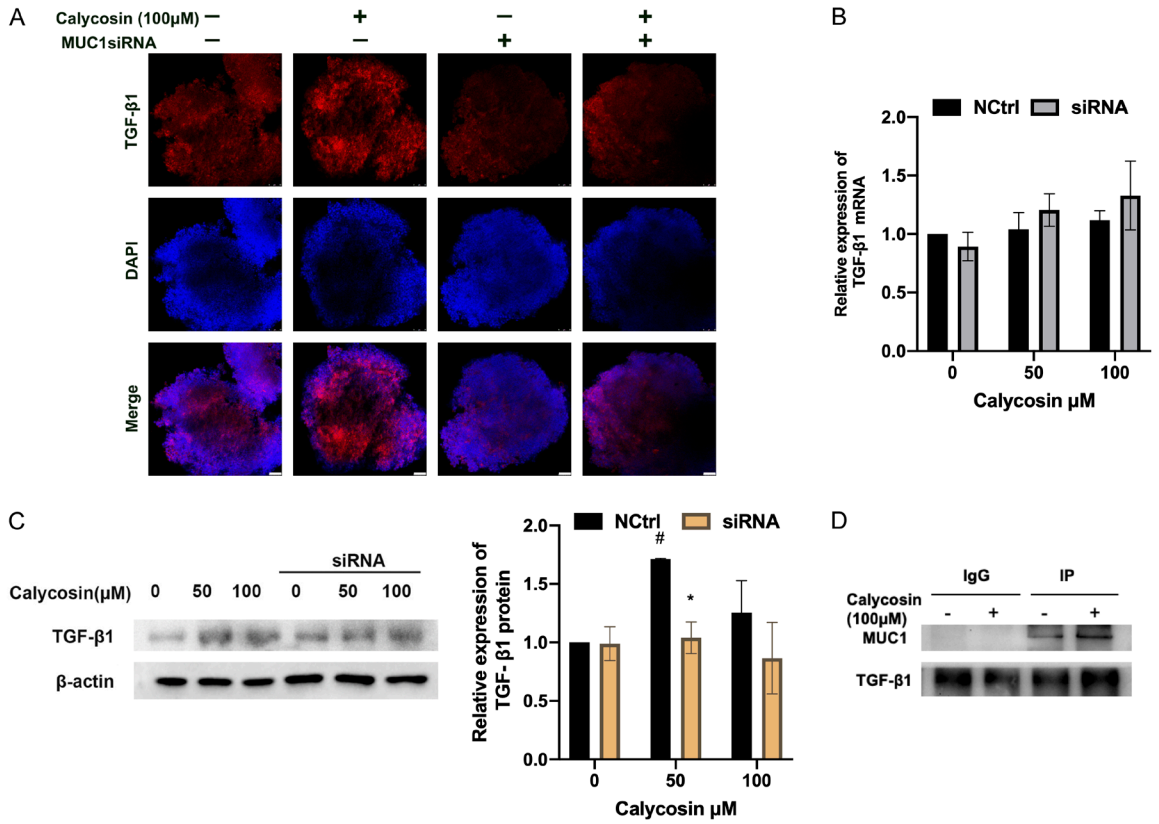


**Figure 3.** Effects of calycosin on the expression of TGF-β1 (with or without MUC1 gene silencing). Immunofluorescence staining of TGF-β1 (green) in MIA-PaCa2 cells treated with 100 μM calycosin for 24 h using (A) 3D cell culture (scale bar is 50 μm). The nuclei were stained with DAPI (blue). Magnifications: 20× for 3D cell culture. (B) Gene expression of TGF-β1 in MIA PaCa-2 cells after treatment with calycosin (50 or 100 μM) for 24 h was detected by quantitative reverse transcription PCR. #P<0.05 versus corresponding group without calycosin treatment (0 μM). (C) Protein expression of TGF-β1 in MIA PaCa-2 cells after treatment with calycosin (50 or 100 μM) for 24 h was detected by Western immunoblotting. *P<0.05, **P<0.01, ***P<0.001 versus the corresponding negative control (NCtrl) group. (D) The protein interaction of MUC1 and TGF-β in MIA PaCa-2 cells after treatment with calycosin (100 μM) for 24 h was detected by co-immunoprecipitation and Western immunoblotting. *P<0.05, **P<0.01, ***P<0.001 versus the corresponding negative control (NCtrl) group. #P<0.05, ##P<0.01, ###P<0.0001 versus corresponding group without calycosin treatment (0 μM). Cells treated with DMSO were used as negative control. Data are expressed as mean ± SD from 3 independent experiments.

pression was decreased by calycosin treatment, with further downregulation by MUC1 gene silencing (**Figure 2C**). Calycosin upregulated the protein expression of MUC1 in MIA-PaCa2 cells, which was completely diminished under MUC1 gene silencing (**Figure 2D**). These data have indicated that calycosin would upregulate MUC1 cellular and protein expression but downregulate its gene expression in PDAC cells, with all expression diminished by MUC1 gene silencing.

*MUC1 upregulation by calycosin caused alteration of TGF-β expression in PDAC cells*

To explore whether regulation of MUC1 can affect the expression of TGF-β in PDAC cells, IF assessment in 3D cell cultures was performed (**Figure 3A**). Calycosin treatment (100 μM) for 24 h significantly increased TGF-β expression in PDAC 3D culture. MUC1 gene silencing substantially reduced basal and calycosin-induced TGF-β cell expression level. A similar observation was attained in TGF-β protein expression using Western immunoblotting (**Figure 3C**). However, insignificant alteration in MUC1 gene expression was observed (**Figure 3B**). To further demonstrate whether MUC1 acts directly on TGF-β at the protein level, co-immunoprecipitation (co-IP) was employed to validate the fact that calycosin (100 μM) caused a significant increase in TGF-β expression with corresponding MUC1 upregulation (**Figure 3D**). These data have proven that regulation of TGF-β in PDAC

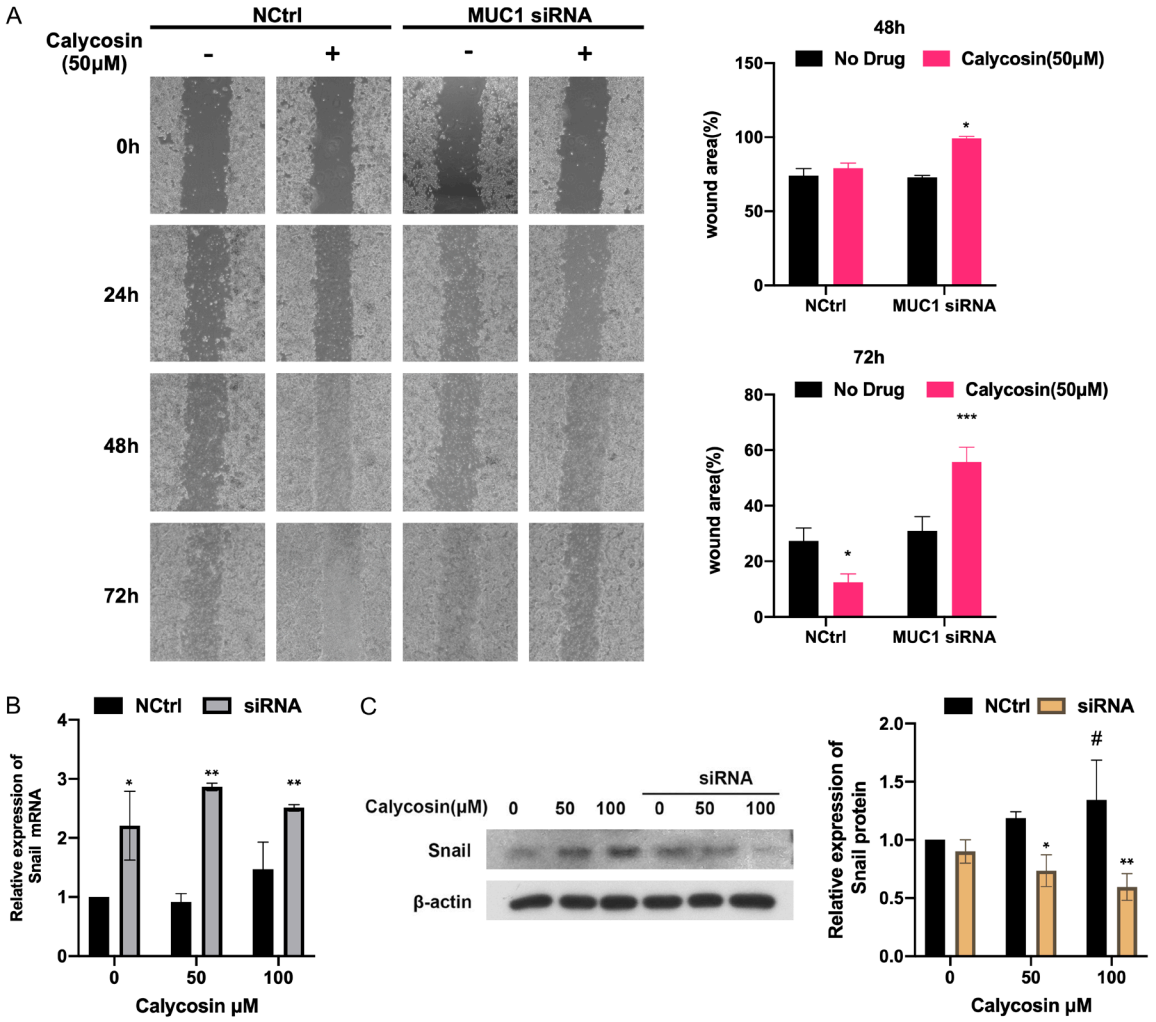


**Figure 4.** Effects of calycosin on the migration of MIA PaCa-2 cells (with or without MUC1 gene silencing). A. Wound healing assay was used in MIA-PaCa2 cells treated with 50 μM calycosin with or without MUC1 siRNA for 0, 24, 48 h or 72 h. Area between the inner margins of migrating cells during wound closure was quantified. Three independent experiments were conducted each in triplicate. Data are presented as mean ± SD. $^{*}$P<0.05, $^{***}$P<0.001 versus the corresponding group without calycosin treatment. B. Gene expression of Snail in MIA PaCa-2 cells after treatment with calycosin (50 or 100 μM) for 24 h was detected by quantitative reverse transcription PCR. $^{*}$P<0.01, $^{**}$P<0.001 versus the corresponding negative control (NCtrl) group. C. Protein expression of Snail in MIA PaCa-2 cells after treatment with calycosin (50 or 100 μM) for 24 h was detected by Western immunoblotting. $^{*}$P<0.01, $^{**}$P<0.001 versus the corresponding negative control (NCtrl) group. $^{\#}$P<0.01 versus corresponding group without calycosin treatment (0 μM). Cells treated with DMSO were used as negative control. Data are expressed as mean ± SD from 3 independent experiments.

cells by calycosin was due to direct MUC1 modulation.

*Calycosin inhibited PDAC cell migration in PDAC cells with MUC1 gene silencing*

Excessive cell migratory activity is one of the hallmarks of malignant tumors. By using a wound healing assay, it was shown that calycosin produce a significant effect after 72 hours of treatment, and the "wound area" was significantly increased by the drug under MUC1 gene silencing, designating an inhibition of PDAC cell migration (**Figure 4A**). The expression level of epithelial mesenchymal transition (EMT) transcription factor Snail (Zinc finger protein SNAI1) was then examined. Calycosin treatment for 24 hours had a tendency to increase the gene and protein expression of Snail (attaining a significant level in protein expression at the higher drug concentration), which

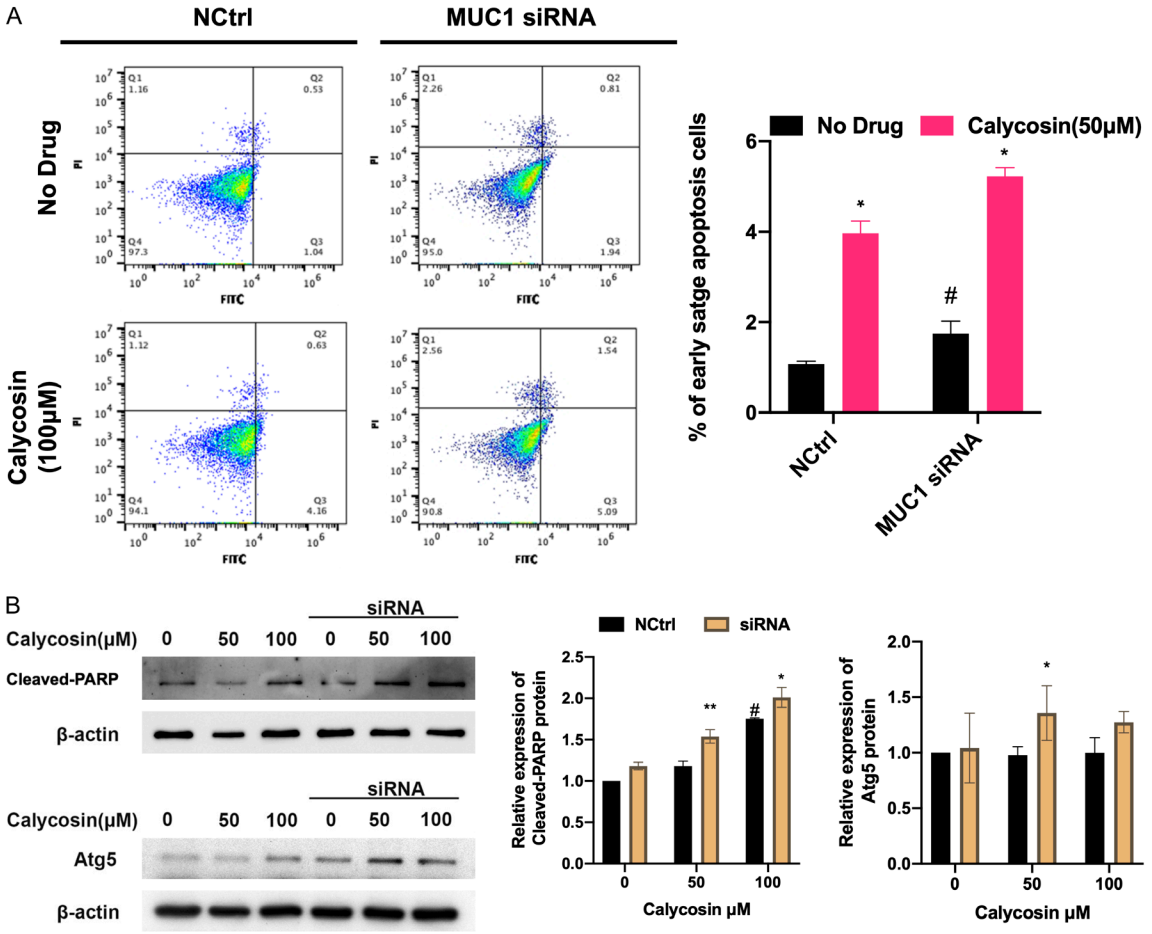


**Figure 5.** Effects of calycosin on the apoptosis of MIA-PaCa2 cells (with or without MUC1 gene silencing). A. FITC/PI staining was performed in MIA-PaCa2 cells treated with 50 μM calycosin with or without MUC1 siRNA for 24 h. Three independent experiments were performed each in triplicate. *P<0.01, **P<0.001 versus the corresponding group without calycosin treatment (No drug). #P<0.01 versus corresponding group without calycosin treatment (0 μM). B. Protein expression of Cleaved-PARP and Atg5 in MIA PaCa-2 cells after treatment with calycosin (50 or 100 μM) for 24 h was detected by Western immunoblotting. *P<0.05, **P<0.01 versus the corresponding negative control (NCtrl) group. #P<0.05 versus corresponding group without calycosin treatment (0 μM). Cells treated with DMSO were used as negative control. Data are expressed as mean ± SD from 3 independent experiments.

was reciprocally regulated following MUC1 gene silencing (**Figure 4B**, **4C**). These data suggest that PDAC cell migration could be inhibited by calycosin under MUC1 gene silencing through downregulation of EMT biomarker Snail at the protein level.

*Calycosin promoted apoptosis under MUC1 gene silencing in PDAC cells*

Through FITC Annexin V/PI staining using flow cytometry, it was shown that calycosin significantly induced early apoptosis, which was further promoted under MUC1 gene silencing (**Figure 5A**). The apoptosis marker cleaved-nuclear poly (ADP-ribose) polymerase (PARP) was overexpressed in protein level with calycosin treatment and became more overexpressed when MUC1 gene silencing (**Figure 5B**). Autophagy can activate cell apoptosis [26], thus the autophagy factor Atg5 (autophagy-related 5) was also assessed. Knockdown of the MUC1 gene upregulated protein expression of Atg5, although the drug did not cause a significant alteration in the negative control group with basal MUC1 level (**Figure 5B**). These results suggest that with MUC1 gene silencing, induction of apoptosis by calycosin would be further promoted in PDAC cells, with a definite contribution by the activation of autophagy.

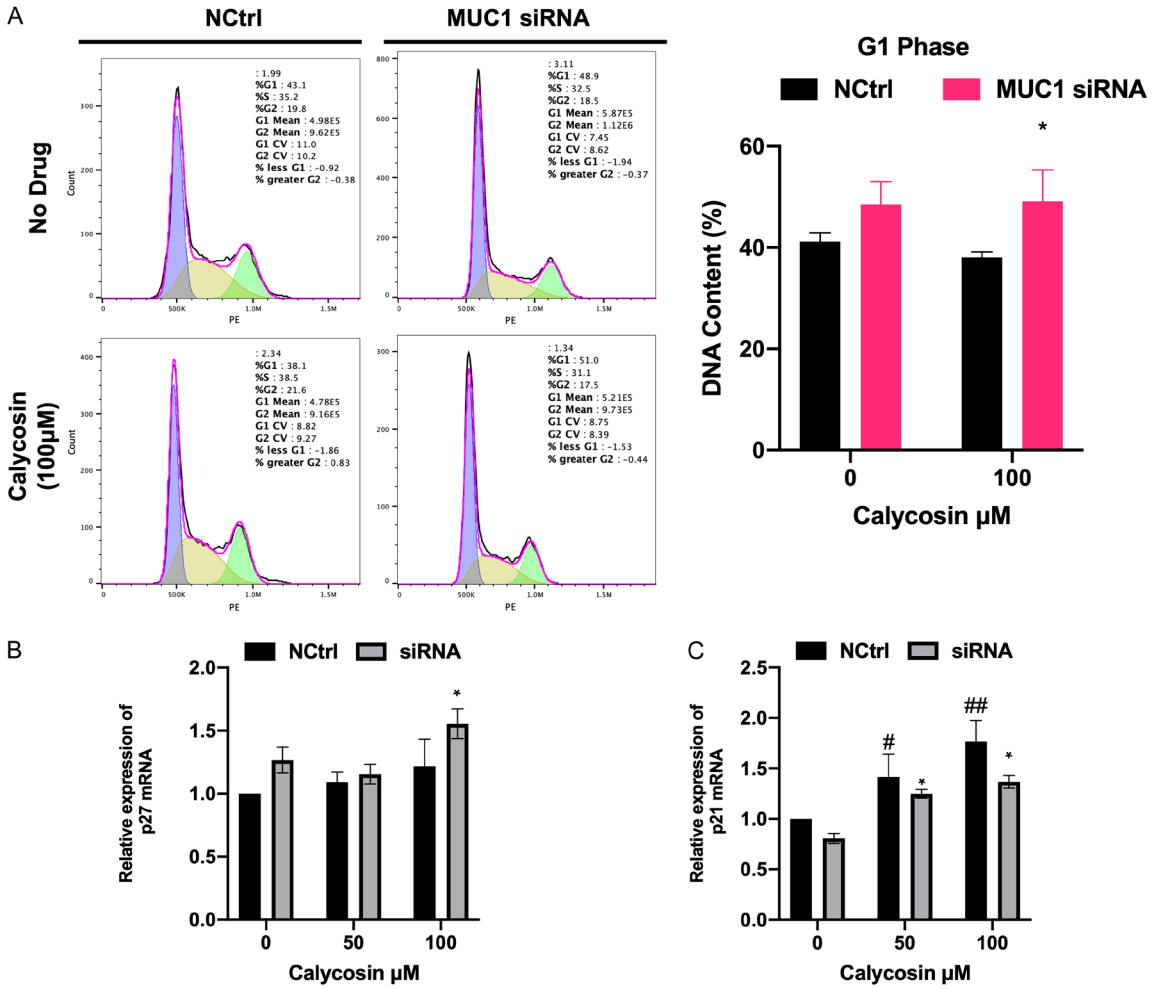


**Figure 6.** Effects of calycosin on cell cycle modulation in MIA-PaCa2 cells (with or without MUC1 gene silencing). (A) Cell cycle analysis was performed in MIA-PaCa2 cells treated with 100 μM calycosin with or without MUC1 siRNA for 24 h. Gene expression of (B) p27 and (C) p21 in MIA PaCa-2 cells after treatment with calycosin (50 or 100 μM) for 24 h was detected by quantitative reverse transcription PCR. Cells treated with DMSO were used as negative control. Data are expressed as mean ± SD from 3 independent experiments. $^{*}$P<0.05 versus the corresponding negative control (NCtrl) group. $^{\#}$P<0.01, $^{\#\#}$P<0.001, $^{\#\#\#}$P<0.0001 versus corresponding group without calycosin treatment (0 μM).

*Calycosin alleviated the G1 phase arrest caused by MUC1 gene silencing in PDAC cells*

Induction of apoptosis is often preceded by changes in cell cycle kinetics, thus cell cycle alteration in MIA-PaCa2 cells by calycosin under different MUC1 gene expression levels was examined by flow cytometry. Calycosin or MUC1 siRNA itself could not significantly modulate the cell cycle. Nevertheless, accumulation of cells at G1 phase (from 41.87±2.125% to 48.533±3.433%) in the calycosin treatment group under MUC1 gene silencing (**Figure 6A**), designated induction of cell cycle arrest at G1-S transition. In addition, gene expression of the cell cycle regulators p27 (cyclin-dependent kinase inhibitor 1B) and p21 (cyclin-dependent kinase inhibitor 1) was also assessed (**Figure 6B**, **6C**). Results indicate an increasing tendency of p27 and p21 mRNA expression after calycosin treatment (statistically significant for p21). With MUC1 gene silencing, calycosin-induced p27 gene expression became significantly upregulated, with a recipricol attenuation of p21 expression. Here, the suppression of p21 gene expression by calycosin under MUC1 gene silencing could be interpreted as a pro-apoptotic manifestation of p21 that had also been reported in one of our previous studies [27]. These findings provide us with the

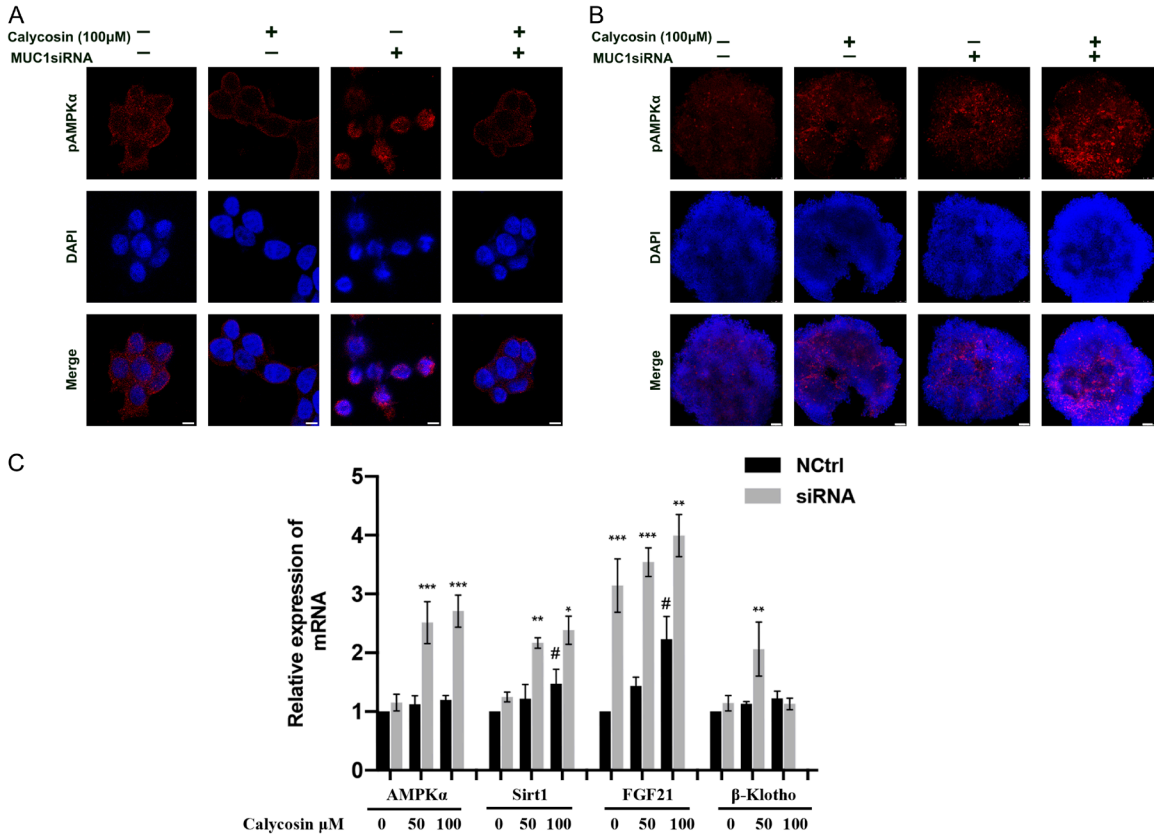


**Figure 7.** Effects of calycosin on metabolic regulation in MIA PaCa2 cells (with or without MUC1 gene silencing). Immunofluorescence staining of AMPKα (red) in MIA-PaCa2 cells treated with 100 μM calycosin for 24 h using (A) 2D or (B) 3D cell culture. The nuclei were stained with DAPI (blue). Magnifications: 60× for 2D cell culture (The scale bar is 5 μm); 20× for 3D cell culture (The scale bar is 50 μm). (C) Gene expression of AMPKα, Sirt1, FGF21 and β-klotho in MIA PaCa-2 cells after treatment with calycosin (50 or 100 μM) for 24 h was detected by quantitative reverse transcription PCR. Cells treated with DMSO were used as negative control. Data are expressed as mean ± SD from 3 independent experiments. $^{*}$P<0.05, $^{**}$P<0.01, $^{***}$P<0.0001 versus the corresponding negative control (NCtrl) group. $^{\#}$P<0.05, $^{\#\#}$P<0.01, $^{\#\#\#}$P<0.0001 versus corresponding group without calycosin treatment (0 μM).

insight that MUC1 gene knockdown can induce phase-specific cell cycle arrest in MIA-PaCa2 cells through differential modulation of the growth-regulatory genes, being concurrently regulated by calycosin.

*Calycosin facilitated metabolic regulation of PDAC under MUC1 gene silencing*

The Energy metabolic profile of tumor cells has exhibited a remarkable correlation with FGF21/β-klotho signaling, which in turn involves the AMPKα pathway. Marked activation of AMPKα by calycosin was shown in the 3D culture of MIA-PaCa2 cells, with further increase following MUC1 gene silencing (**Figure 7B**). Nonetheless, calycosin treatment did not alter the gene expression of the metabolic regulators AMPKα and β-klotho, while significantly upregulated Sirt1 and FGF21 expression (**Figure 7C**). Under MUC1 gene silencing, calycosin was capable of upregulating the gene expression level of all metabolic regulators being tested. These findings implicate that calycosin promotes metabolic regulation in PDAC cells which becomes more prominent with MUC1 gene silencing.

*Calycosin increased tumor tissue expression of MUC1 in mice xenografted with pancreatic cancer cells*

In our recent study, we have envisaged that calycosin may promote EMT and polarization of M2 macrophages through TGF-β activation [28]. Here, we further explored the drug effect on MUC1 expression *in vivo* in a tumor xenograft model using C57/BL6 mice. On top of the

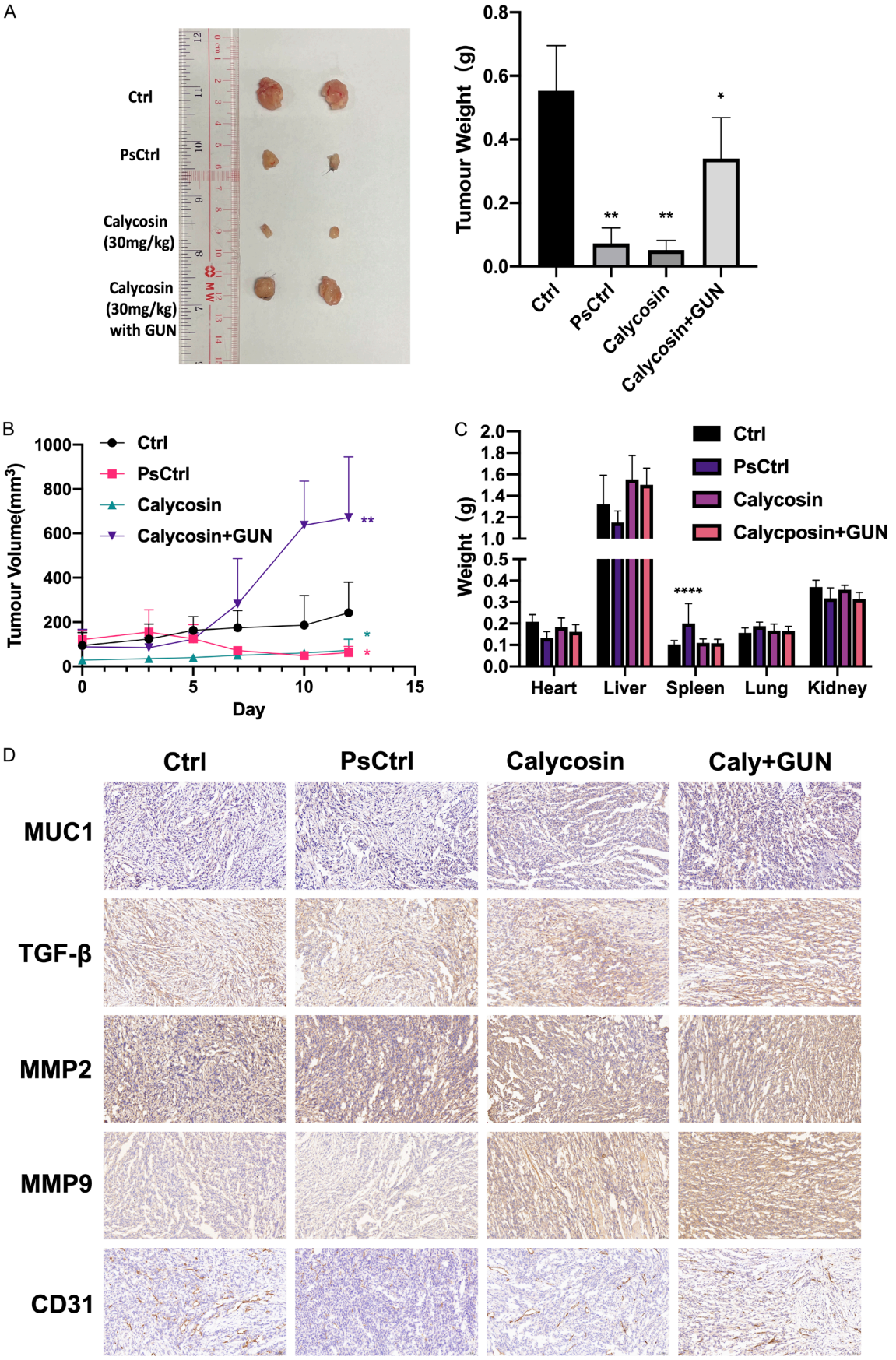
A
Ctrl
PsCtrl
Calycosin (30mg/kg)
Calycosin (30mg/kg) with GUN
Tumour Weight (g)
0.8
0.6
0.4
0.2
0.0
**
**
*
Ctrl
PsCtrl
Calycosin
Calycosin+GUN
B
Tumour Volume(mm3)
1000
800
600
400
200
0
Ctrl
PsCtrl
Calycosin
Calycosin+GUN
**
*
*
0
5
10
15
Day
C
Weight (g)
2.0
1.8
1.6
1.4
1.2
1.0
0.5
0.4
0.3
0.2
0.1
0.0
Ctrl
PsCtrl
Calycosin
Calycposin+GUN
****
Heart
Liver
Spleen
Lung
Kidney
D
Ctrl
PsCtrl
Calycosin
Caly+GUN
MUC1
TGF-β
MMP2
MMP9
CD31

**Figure 8.** The effect of calycosin in PDAC tumor-bearing C57/BL6 mice. A. Calycosin exerted anti-tumor effect in Pan02 tumor-bearing C57/BL6 mice. Ctrl: PBS, PsCtrl: gemcitabine 30 mg/kg i.p. every other day, calcyosin: 30 mg/kg once daily, calycosin + Gun: 100V electroporation for 12 days. More than 80% reduction in tumor mass. B. Daily change of tumor volume over 12 days. Tumor volume of PsCtrl and calycosin groups were decreased, with increase in calycosin + Gun group. C, D. IHC assays of tissues for MUC1, TGF-β, MMP2, MMP9 and CD31 in different treatment groups (magnification =20×).

drug treatment groups, electroporation was conducted in an additional calycosin treatment group. Results indicate that 30 mg/kg calycosin significantly inhibited tumor growth in mice by more than 80%, which had a slightly better tumor-suppressive effect when compared with that caused by the chemotherapeutic drug gemcitabine (**Figure 8A**). Surprisingly, the tumor-suppressive effect of calycosin was largely diminished with concurrent electroporation treatment. No significant weight loss was observed in the calycosin or calycosin with electroporation treatment groups, suggesting that no systemic toxicity was evoked (**Figure 8B**). There was also no hepatic or renal toxicity being observed according to the organ index plots of various drug treatment groups and the group involving electroporation (**Figure 8C**). To extrapolate from our *in vitro* data on calycosin drug action in the promotion of EMT through TGF-β activation, we further discovered that tissue expression of both MUC1 and TGF-β1 was significantly upregulated in tumor sections obtained from the xenograft mice model following calycosin treatment. This phenomenon was exaggerated by simultaneous electroporation (**Figure 8D**). Besides, the tissue expression of matrix metallopeptidases (MMP) 2, MMP9 and CD31 (cluster of differentiation 31) in PDAC cells was upregulated by calycosin treatment, indicating the tendency to promote EMT. Likewise, these properties were further amplified with concurrent electroporation (**Figure 8D**). All these findings implicate that the drive for cell invasiveness and angiogenesis by calycosin could be amplified by electroporation, contributing to the earlier observation of tumor growth aggravation.

## Discussion

Surgical removal of the tumor remains the most effective treatment approach in pancreatic cancer therapy. However, when the tumor starts to metastasize, resection may no longer be meaningful for most pancreatic cancer patients. Besides, the high rate of chemoresistance against gemcitabine, the first-line chemotherapeutic drug treatment in non-resectable cases also contributes to the low survival rate, which has prompted the urge to explore alternative neoadjuvant chemotherapeutic agents. In our ongoing study [6], a potential anticancer agent calycosin has demonstrated excellent growth inhibition but also possesses a pro-metastatic tendency when treating pancreatic cancer. We postulated that such a phenomenon could be due to the dual properties of its regulator TGF-β as both tumor suppressor and metastatic promoter [28]. Through network pharmacology, we have deciphered that the most potential common gene target between *Astragalus* constituents and PDAC is MUC1, which is an oncogene found to be overexpressed in various human cancer cell types, including pancreatic cancer. In this study, we have explored the crucial role played by MUC1 in the pharmacological effects of calycosin and its interaction with TGF-β in PDAC. MUC1 and TGF-β expression in PDAC cells was concomitantly upregulated following calycosin treatment as shown in the immunofluorescence microscopic pictures. This phenomenon is supported by the earlier report from Grover et al. [25], which stated that overexpression of MUC1 can activate TGF-β that could subsequently promote migration and invasion in pancreatic cancer. We further envisaged that MUC1 gene silencing could downregulate the protein expression of TGF-β in PDAC cells. Calycosin could suppress the migration of PDAC cells only with MUC1 gene knock-down. Snail is the molecular biomarker mastering EMT, an essential participant in tumor invasion and metastasis [29]. The protein expression of Snail was concentration-dependently downregulated in calycosin-treated cells under MUC1 silencing despite a surge in its gene expression. Hence, the anti-migratory activity of calycosin should act via EMT regulation under MUC1 knockout. We cannot explain the enigmatic increase in Snail gene expression, but it is known that the predictive correlation between genes of regulation and their respective proteins are relatively low [30], of which an unusual pattern of reciprocal mRNA and protein expression may sometimes be possible [31].

Other than the alleviation of cell invasiveness, a profound modulation of the cell cycle and induction of early-stage apoptosis together with metabolic regulation could be facilitated by calycosin in PDAC cells when the MUC1 gene was knockdown. Moreover, regulation of p27, p21, cleaved-PARP and Atg5 further verified these. p27 is a known cell cycle regulator through inhibition at the G1/S boundary in response to the anti-proliferative signal, while its CDK-independent activities may also involve in other cellular processes like cell motility control, activation of apoptosis and autophagy, all contributing to cancer progression and metastasis [32]. p27 mRNA is overexpressed in many cancer cells to promote apoptosis [32], while p21 could be associated with anti-apoptotic activities [33]. Our findings in p27 and p21 expression implicate that under MUC1 gene knockdown, the potential of calycosin to promote cell cycle regulation and apoptosis in PDAC cells will be enhanced. Alternatively, although p27 is a cell cycle regulator, it also possesses CDK-independent activities involved in modulating cytoskeleton dynamics control, apoptosis and autophagy activation [34], some of which could be oncogenic to facilitate cancer progression and metastasis. In autophagy, p27 can act as the substrate of AMPKα, a key energy-controlling enzyme [32]. To confirm this rationale, we then tested the typical biomarkers of apoptosis cleaved-PARP, one of key cell substrates, which promotes cell disassembly and induces to apoptosis [35]. Also, we tested the autophagy-related molecule Atg5, which can accelerate autophagy as well as generate precursors of the protein upon caspase activation to stimulate apoptosis [26]. Our results indicate that under MUC1 gene silencing, the protein expression of Atg5 was increased to different extents in PDAC cells, further implicating the promotion of apoptosis by the drug. With respect to the cell cycle, p21 can be activated by the tumor suppressor p53 that subsequently triggers momentary G1 phase arrest upon DNA damage or other stressors [36]. With MUC1 knockdown, this condition would be exaggerated, which can be supported by the increase of p27 mRNA expression [32, 37]. In the context of metabolic regulation, AMPKα is a key molecule responsible for energy regulation. The AMPKα-Sirt1-FGF21 cascade has a strong correlation to metabolic energy modulation. FGF21 can enhance the expression of enzymes in mitochondrial metabolism and improve the mitochondrial respiratory capacity of adipocytes through the AMPK-Sirt1 pathway [38]. Besides, FGF21 and AMPK activation can both increase glucose uptake and decrease hyperglycaemia by promoting energy expenditure, together with the increase in insulin sensitivity to attenuate metabolic stresses [39-44]. In PDAC, loss of FGF21 due to the expression of mutant oncogenic K-Ras may lead to a metabolic vulnerability [23]. Our data has shown that AMPKα, Sirt1, FGF21 and β-Klotho were all augmented significantly following calycosin treatment when the MUC1 gene was knockdown in PDAC, which designates the importance of MUC1 in the action of calycosin to modulate energy metabolism in treating PDAC.

In the PDAC tumor xenograft model using C57/BL6 mice, calycosin has demonstrated no systemic toxicity, which was in contrast to the case of gemcitabine. Calycosin treatment alone could effectively reduce the size of PDAC tumors to a similar degree as gemcitabine. However, with concurrent electroporation, a procedure that could facilitate better drug targeting to tumor tissues, the tumor size was increased instead. MUC1 and TGF-β expression was downregulated by calycosin at the gene level but showing increment otherwise in the tumor tissue level, with further augmentation with concurrent electroporation. In addition, calycosin promoted the protein expression of MMP9 and CD31, which are important pro-invasive and angiogenic markers closely associated with tumor metastasis. Enhanced expression of MUC1, MMP9 and CD31 with concurrent electroporation may explain the metastatic-promoting drive in PDAC. These results suggest that calycosin can effectively reduce tumor size and reduce metabolic regulation but may promote angiogenesis, possibly due to its estrogenic property. Furthermore, when calycosin was administered together with electroporation procedure to enhance drug targeting, its metastasis-promoting potential becomes predominated through its pro-angiogenic characteristic that could lead to the reversal of energy metabolism regulation - an idea that needs to be justified in the prospective study.

Taken together, modulation of the oncogene MUC1 is a crucial part of PDAC treatment, which may help to explain why calycosin dis-

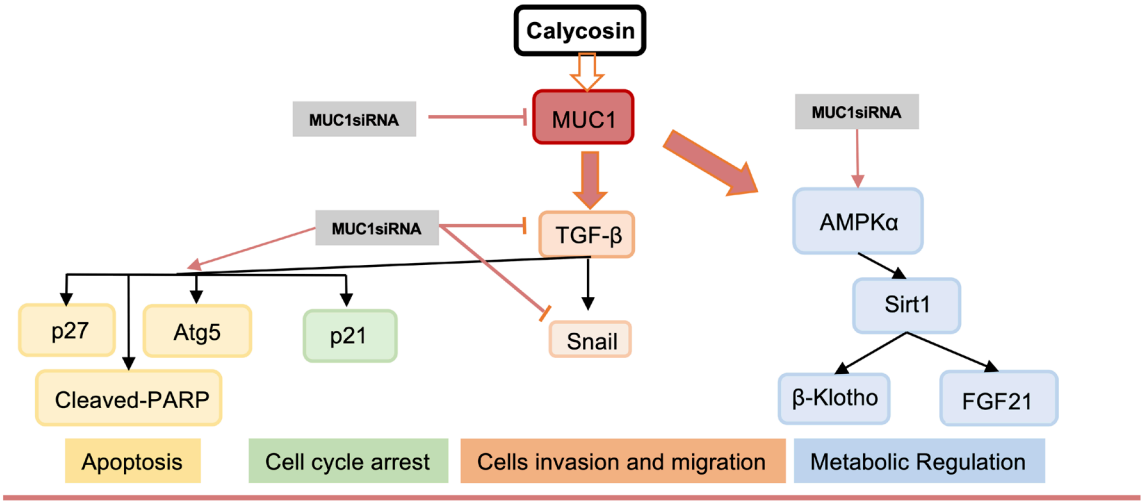


**Figure 9.** The mechanism of MUC1 in treating PDAC by calycosin.

plays dual tendencies of growth inhibition and metastatic progression in pancreatic cancer treatment. Rectification of the pro-metastatic potential of calycosin by MUC1 knockdown could help to alleviate the tumor-promoting nature of TGF-β. With MUC1 gene knockdown, calycosin effectively inhibits pancreatic cancer cell invasion through EMT regulation, promotes cell cycle arrest and early-stage apoptosis via induction of autophagy, as well as facilitates metabolic regulation in PDAC. It has been reported that several MUC1-associated proliferation signature genes could be used to predict treatment outcome that affects patient survival [45]. Among these, RRM has been found in our heatmap as another common potential gene target between PDAC and *Astragalus* constituents (**Figure 1F**) that is currently under our investigation. The complete mechanistic roadmap of calycosin associated with the MUC1 gene and the downstream signaling pathways is summarized in **Figure 9**. It is remarkable that by genetic suppression of MUC1, calycosin can be adopted as a potential anti-tumorigenic neoadjuvant in the treatment of pancreatic cancer that is free from the metastatic drive and systemic toxicity.

## Acknowledgements

This study was supported by the Hong Kong Baptist University Faculty Research Grant FRG1/17-18/012 and the Guangdong Basic and Applied Basic Research Foundation, grant number: No. 2021A1515012092.

## Disclosure of conflict of interest

None.

**Address correspondence to:** Joshua Ka-Shun Ko and Ken Kin-Lam Yung, Jockey Club School of Chinese Medicine Building, Hong Kong Baptist University, 7 Baptist University Road, Kowloon Tong, Kowloon, Hong Kong SAR, China. Tel: +852-3411-2907; Fax: +852-3411-2461; E-mail: jksko@hkbu.edu.hk (JKSK); Tel: +852-3411-7060; Fax: +852-3411-5995; E-mail: kklyung@hkbu.edu.hk (KKLY)

## References

[1] Siegel RL, Miller KD and Jemal A. Cancer statistics, 2020. CA Cancer J Clin 2020; 70: 7-30.

[2] Rahib L, Smith BD, Aizenberg R, Rosenzweig AB, Fleshman JM and Matrisian LM. Projecting cancer incidence and deaths to 2030: the unexpected burden of thyroid, liver, and pancreas cancers in the United States. Cancer Res 2014; 74: 2913-2921.

[3] Ren B, Liu XY and Suriawinata AA. Pancreatic ductal adenocarcinoma and its precursor lesions: histopathology, cytopathology, and molecular pathology. Am J Pathol 2019; 189: 9-21.

[4] Malinda RR, Zeeberg K, Sharku PC, Ludwig MQ, Pedersen LB, Christensen ST and Pedersen SF. TGFbeta signaling increases net acid extrusion, proliferation and invasion in Panc-1 pancreatic cancer cells: SMAD4 dependence and link to Merlin/NF2 signaling. Front Oncol 2020; 10: 687.

[5] Gao JQ, Liu ZJ, Chen T and Zhao DQ. Pharmaceutical properties of calycosin, the major

bioactive isoflavonoid in the dry root extract of Radix astragali. Pharm Biol 2014; 52: 1217-1222.
[6] Zhang Z, Auyeung KK, Sze SC, Zhang S, Yung KK and Ko JK. The dual roles of calycosin in growth inhibition and metastatic progression during pancreatic cancer development: a "TGF-β paradox". Phytomedicine 2020; 68: 153177.
[7] Nath S and Mukherjee P. MUC1: a multifaceted oncoprotein with a key role in cancer progression. Trends Mol Med 2014; 20: 332-342.
[8] Li QS, Liu GM, Shao D, Wang J, Yuan HY, Chen TX, Zhai RP, Ni WH and Tai GX. Mucin1 mediates autocrine transforming growth factor beta signaling through activating the c-Jun N-terminal kinase/activator protein 1 pathway in human hepatocellular carcinoma cells. Int J Biochem Cell Biol 2015; 59: 116-125.
[9] Apostolopoulos V, Pietersz GA, Tsibanis A, Tsikkinis A, Drakaki H, Loveland BE, Piddlesden SJ, Plebanski M, Pouniotis DS, Alexis MN, McKenzie IF and Vassilaros S. Pilot phase III immunotherapy study in early-stage breast cancer patients using oxidized mannan-MUC1 [ISRCTN71711835]. Breast Cancer Res 2006; 8: R27.
[10] Kufe DW. Mucins in cancer: function, prognosis and therapy. Nat Rev Cancer 2009; 9: 874-885.
[11] Sugiura D, Aida S, Denda-Nagai K, Takeda K, Kamata-Sakurai M, Yagita H and Irimura T. Differential effector mechanisms induced by vaccination with MUC1 DNA in the rejection of colon carcinoma growth at orthotopic sites and metastases. Cancer Sci 2008; 99: 2477-2484.
[12] Roy LD, Sahraei M, Subramani DB, Besmer D, Nath S, Tinder TL, Bajaj E, Shanmugam K, Lee YY, Hwang SI, Gendler SJ and Mukherjee P. MUC1 enhances invasiveness of pancreatic cancer cells by inducing epithelial to mesenchymal transition. Oncogene 2011; 30: 1449-1459.
[13] Wang J, Liu GM, Li QS, Wang F, Xie F, Zhai RP, Guo YY, Chen TX, Zhang NN, Ni WH, Yuan HY and Tai GX. Mucin1 promotes the migration and invasion of hepatocellular carcinoma cells via JNK-mediated phosphorylation of Smad2 at the C-terminal and linker regions. Oncotarget 2015; 6: 19264-19278.
[14] Bozkaya G, Korhan P, Cokaklı M, Erdal E, Sağol O, Karademir S, Korch C and Atabey N. Cooperative interaction of MUC1 with the HGF/c-Met pathway during hepatocarcinogenesis. Mol Cancer 2012; 11: 64.
[15] Li QS, Wang FL, Liu GM, Yuan HY, Chen TX, Wang J, Xie F, Zhai RP, Wang F, Guo YY, Ni WH and Tai GX. Impact of Mucin1 knockdown on the phenotypic characteristics of the human hepatocellular carcinoma cell line SMMC-7721. Oncol Rep 2014; 31: 2811-2819.
[16] Li Y, Kuwahara H, Ren J, Wen G and Kufe D. The c-Src tyrosine kinase regulates signaling of the human DF3/MUC1 carcinoma-associated antigen with GSK3 beta and beta-catenin. J Biol Chem 2001; 276: 6061-6064.
[17] Pandey P, Kharbanda S and Kufe D. Association of the DF3/MUC1 breast cancer antigen with Grb2 and the Sos/Ras exchange protein. Cancer Res 1995; 55: 4000-4003.
[18] Wei XL, Xu H and Kufe D. Human mucin 1 oncoprotein represses transcription of the p53 tumor suppressor gene. Cancer Res 2007; 67: 1853-1858.
[19] Huang L, Chen DS, Liu D, Yin L, Kharbanda S and Kufe D. MUC1 oncoprotein blocks glycogen synthase kinase 3beta-mediated phosphorylation and degradation of beta-catenin. Cancer Res 2005; 65: 10413-10422.
[20] Lau SK, Shields DJ, Murphy EA, Desgrosellier JS, Anand S, Huang M, Kato S, Lim ST, Weis SM, Stupack DG, Schlaepfer DD and Cheresh DA. EGFR-mediated carcinoma cell metastasis mediated by integrin alphavbeta5 depends on activation of c-Src and cleavage of MUC1. PLoS One 2012; 7: e36753.
[21] Schroeder JA, Thompson MC, Gardner MM and Gendler SJ. Transgenic MUC1 interacts with epidermal growth factor receptor and correlates with mitogen-activated protein kinase activation in the mouse mammary gland. J Biol Chem 2001; 276: 13057-13064.
[22] Wang J, Ni WH, Hu KB, Zhai XY, Xie F, Jie J, Zhang NN, Jiang LN, Yuan HY and Tai GX. Targeting MUC1 and JNK by RNA interference and inhibitor inhibit the development of hepatocellular carcinoma. Cancer Sci 2017; 108: 504-511.
[23] Luo YD, Ye S, Chen X, Gong FH, Lu WQ and Li XK. Rush to the fire: FGF21 extinguishes metabolic stress, metaflammation and tissue damage. Cytokine Growth Factor Rev 2017; 38: 59-65.
[24] Yi FT and Lu QP. Mucin 1 promotes radioresistance in hepatocellular carcinoma cells through activation of JAK2/STAT3 signaling. Oncol Lett 2017; 14: 7571-7576.
[25] Grover P, Nath S, Nye MD, Zhou R, Ahmad M and Mukherjee P. SMAD4-independent activation of TGF-β signaling by MUC1 in a human pancreatic cancer cell line. Oncotarget 2018; 9: 6897-6910.
[26] Marino G, Niso-Santano M, Baehrecke EH and Kroemer G. Self-consumption: the interplay of autophagy and apoptosis. Nat Rev Mol Cell Biol 2014; 15: 81-94.
[27] Auyeung KK, Woo PK, Law PC and Ko JK. Astragalus saponins modulate cell invasiveness

and angiogenesis in human gastric adenocarcinoma cells. J Ethnopharmacol 2012; 141: 635-641.
[28] Akhurst RJ and Derynck R. TGF-β signaling in cancer-a double-edged sword. Trends Cell Biol 2001; 11: S44-S51.
[29] Xu SS, Zhou YX, Biekemitoufu H, Wang H, Li C, Zhang WJ and Ma YQ. Expression of Twist, Slug and Snail in esophageal squamous cell carcinoma and their prognostic significance. Oncol Lett 2021; 21: 184.
[30] Guo YF, Xiao P, Lei SF, Deng FY, Xiao GG, Liu YZ, Chen XD, Li LM, Wu S, Chen Y, Jiang H, Tan LJ, Xie JY, Zhu XZ, Liang SP and Deng HW. How is mRNA expression predictive for protein expression? A correlation study on human circulating monocytes. Acta Biochim Biophys Sin (Shanghai) 2008; 40: 426-436.
[31] Doyle M and Dorman CJ. Reciprocal transcriptional and posttranscriptional growth-phase-dependent expression of sfh, a gene that encodes a paralogue of the nucleoid-associated protein H-NS. J Bacteriol 2006; 188: 7581-7591.
[32] Bencivenga D, Caldarelli I, Stampone E, Mancini FP, Balestrieri ML, Della Ragione F and Borriello A. p27(Kip1) and human cancers: a reappraisal of a still enigmatic protein. Cancer Lett 2017; 403: 354-365.
[33] Chang BD, Watanabe K, Broude EV, Fang J, Poole JC, Kalinichenko TV and Roninson IB. Effects of p21Waf1/Cip1/Sdi1 on cellular gene expression: implications for carcinogenesis, senescence, and age-related diseases. Proc Natl Acad Sci U S A 2000; 97: 4291-4296.
[34] Binenbaum Y, Na'ara S and Gil Z. Gemcitabine resistance in pancreatic ductal adenocarcinoma. Drug Resist Updat 2015; 23: 55-68.
[35] Oliver FJ, de la Rubia G, Rolli V, Ruiz-Ruiz MC, de Murcia G and Murcia JM. Importance of poly (ADP-ribose) polymerase and its cleavage in apoptosis. Lesson from an uncleavable mutant. J Biol Chem 1998; 273: 33533-33539.
[36] Georgakilas AG, Martin OA and Bonner WM. p21: a two-faced genome guardian. Trends Mol Med 2017; 23: 310-319.
[37] Abbastabar M, Kheyrollah M, Azizian K, Bagherlou N, Tehrani SS, Maniati M and Karimian A. Multiple functions of p27 in cell cycle, apoptosis, epigenetic modification and transcriptional regulation for the control of cell growth: a double-edged sword protein. DNA Repair (Amst) 2018; 69: 63-72.
[38] Chau MD, Gao JP, Yang Q, Wu ZD and Gromada J. Fibroblast growth factor 21 regulates energy metabolism by activating the AMPK-SIRT1-PGC-1alpha pathway. Proc Natl Acad Sci U S A 2010; 107: 12553-12558.
[39] Salminen A, Kauppinen A and Kaarniranta K. FGF21 activates AMPK signaling: impact on metabolic regulation and the aging process. J Mol Med (Berl) 2017; 95: 123-131.
[40] Lage R, Diéguez C, Vidal-Puig A and López M. AMPK: a metabolic gauge regulating whole-body energy homeostasis. Trends Mol Med 2008; 14: 539-549.
[41] Woo YC, Xu AM, Wang Y and Lam KS. Fibroblast growth factor 21 as an emerging metabolic regulator: clinical perspectives. Clin Endocrinol (Oxf) 2013; 78: 489-496.
[42] Giralt M, Gavaldà-Navarro A and Villarroya F. Fibroblast growth factor-21, energy balance and obesity. Mol Cell Endocrinol 2015; 418 Pt 1: 66-73.
[43] Camporez JP, Jornayvaz FR, Petersen MC, Pesta D, Guigni BA, Serr J, Zhang D, Kahn M, Samuel VT, Jurczak MJ and Shulman GI. Cellular mechanisms by which FGF21 improves insulin sensitivity in male mice. Endocrinology 2013; 154: 3099-3109.
[44] Ruderman NB, Carling D, Prentki M and Cacicedo JM. AMPK, insulin resistance, and the metabolic syndrome. J Clin Invest 2013; 123: 2764-2772.
[45] MacDermed DM, Khodarev NN, Pitroda SP, Edwards DC, Pelizzari CA, Huang L, Kufe DW and Weichselbaum RR. MUC1-associated proliferation signature predicts outcomes in lung adenocarcinoma patients. BMC Med Genomics 2010; 3: 16.